Catal Lett (2007) 118:211–218
DOI 10.1007/s10562-007-9164-z

The Production of Straight Carbon Microfibers by the Cracking of Methane over Co-SBA-15 Catalysts

Lizen Z. Gao · Sibudjing Kawi

Received: 30 March 2007 / Accepted: 11 June 2007 / Published online: 11 July 2007

Abstract Cobalt incorporated SBA-15 (Co-SBA-15) catalysts were prepared by using hydrothermal synthesis and over which very straight carbon microfibers were made by cracking CH_4. The influence of Co loading (from 0.5 to 3 wt%) in SBA-15 and cracking temperature on the methane conversion, structures and morphologies of the microfibers was investigated. The highest yield of microfibers was obtained at 800 °C over the 2 wt% Co loaded SBA-15 catalyst. After 16 h reaction, the carbon fibers almost stopped further growth. The diameter of the carbon microfibers could be roughly controlled by judiciously adjusting the Co concentration in SBA-15. The carbon microfiber's growth followed a root-growth mechanism. XRD, HRTEM and Raman studies confirmed that the microfibers were graphitic. The microfiber grown over the 0.5 wt% cobalt loaded SBA-15 catalyst had a higher degree of graphitic structural order than that obtained over the 2 wt% cobalt loaded one.

Keywords Co-SBA-15 · Methane cracking · Carbon microfibers · Graphitic carbon

L. Z. Gao (✉)
School of Mechanical Engineering M050, The University of Western Australia, 35 Stirling Highway, Crawley, WA 6009, Australia
e-mail: lizhen@mech.uwa.edu.au

S. Kawi
Department of Chemical and Biomolecular Engineering, National University of Singapore, 4 Engineering Drive 4, Singapore 117576, Republic of Singapore

1 Introduction

The early reports on the production of graphitic filaments including nanofibers can be dated more than a century years ago [1–3]. Initially, the carbon fibers were regarded as an impediment because they blocked the reactors, reduced the heat transfer coefficient and deactivated the catalysts [4, 5]. Carbon nanotubes and fibers did not attract much attention until the 1980s when their extraordinary physical and chemical properties were discovered. Hillert and Lange in 1958 produced carbon nanofilaments exhibiting hollow cavity structures [6]. The interest in fibrous carbon has science then been recurrent [7–9] and a significant boost in the research in carbon nanostructure field coincides with the discovery of multiwalled carbon nanotubes (MWNTs) by lijima [10] and the successive production of single walled carbon nanotubes (SWNTs) [11, 12]. Carbon solid fibers can be derived from several precursors, with polyacrylonitrile (PAN) as the most favored precursor by far for manufacturing high-performance fibers due to the high carbon yield. Vapor-grown carbon fibers (VGCFs) are of great interest to scientific and industrial communities, especially in car and aerospace industry, due to their peculiar properties such as high mechanical strength and good electron transportation [13–15]. VGCFs by the decomposition of hydrocarbons are distinctively different from PAN derived carbon fibers. The former are composed of higher concentration of carbon and are of higher degree of graphitic structure. The growth of carbon micro/nano fibers and nanotubes from hydrocarbon catalytic decomposition is also an important alternative to the carbonization of organic precursors. The organic feedstock, metal catalysts such as Fe, Co and Ni and catalytic process parameters can be tuned to optimize the carbon fibers and tubes [16–20]. Methane is often used as a carbon source because of its low cost, easy handling and scaling up [21]. Even though a lot of efforts have been paid on the growth mechanism revelation of the carbon micro/nano fibers/tubes, the mystery of their generation has not been completely solved. One consensus has been reached, i.e., carbon fibers are grown through the interaction of metal catalyst particles with hydrocarbon vapor at high temperature. The hydrocarbon dissociates at the interface between catalyst and vapor, and carbon atom participates into a graphite trail in the shape of a cylindrical nano tube or fiber [22]. Nørskov et al. observed the MWNT's growing steps over their time resolved, in situ HRTEM facilities and found that that the catalyst particles moved with the growth nanofiber and always stayed at the MWNT's tip. The growth of nanotube was promoted by abrupt shape changes in the catalyst particle itself, which were in turn driven by the reaction between the catalyst and the vapor [23]. The large catalyst particles are inefficient for nanofiber growth. For the very smaller SWNTs the mechanism is far from clear. For SWNT, the catalyst particle is not always seen attached to the nanotube structure. For the growth mechanisms of solid fibers, particularly the solid microfibers, we still know very little. Their formation mechanism may differ from the tube growth. It is interesting to compare the formation process of the carbon solid microfibers and nanotubes, which may lead to well understand the growth nature of fibrous carbon materials. On the other hand, in view of the realistic application, in the near future, the microfibers may be more hopeful than the nanotubes or fibers. For example, the manufacture of microfibrous electrode is viable while the manipulation of nano electrode may have a long way to go. The carbon fibers reported are mostly in coiled features while in application the straight fibers are more expected.

SBA-15 is a purely siliceous phase synthesized in strong acidic media. It is by far the largest pore size mesoporous material with highly ordered hexagonally arranged meso-channels, with thick walls, adjustable pore size from 3 to 30 nm. Its synthesis and utilization have been investigated by many researchers because of its peculiar characteristics such as large internal surface area, uniformity of pore size, easily controlled size of pores, and high thermal stability [24, 25]. It is expected to be useful in the synthesis of ultra fine nanorod arrays, protein separation and highly efficient catalysis [26–30]. The Co/SBA-15 has been used to study the Fischer-Tropsch synthesis. The nanosized cobalt particles (~5.3 nm) were generated in the Co/SBA-15 [31]. Ordered mesoporous carbon has been synthesized by using SBA-15 as template [32]. Nano Pt particles have been supported on SBA-15 for cyclohexene hydrogenation reaction [33]. Another mesoporous material of MCM-41 with uniform mesopore channels varying from about 1.5 to 10 nm has been doped with Co ions. Over Co-MCM-41 catalyst, SWNTs were synthesized [34]. Herein, we report the synthesis of cobalt incorporated SBA-15, over which the very straight carbon microfibers were produced by cracking of methane.

2 Experimental

2.1 Hydrothermal Synthesis of Co-SBA-15

About 2 g of amphiphilic triblock copolymer, poly(ethylene glycol)-*block*-poly(propylene glycol)-*block*-poly(ethylene glycol), was dispersed in 15 g of water and 60 g of 2 M HCl solution while stirring, followed by the addition of 4.25 g of tetraethyl orthosilicate to the homogeneous solution with stirring. $Co(NO_3)_2 \cdot 6H_2O$ and citric acid were then dissolved into the solution and heated at 60 °C with stirring for 1 h. This gel mixture was continuously stirred at 60 °C for 40 h, and finally crystallized in a Teflon-lined autoclave at 100 °C for 2 days. After crystallization the solution product was centrifuged, filtered, washed with de-ionized water, and dried in air at 550 °C for 24 h to decompose the triblock copolymer and obtain a powder (Co-SBA-15). The 0.5 wt% Co-SBA-15, 1 wt% Co-SBA-15, 2 wt% Co-SBA-15 and 3 wt% Co-SBA-15 samples (referred to as $Co_{0.5}$-SBA-15, Co_1-SBA-15, Co_2-SBA-15 and Co_3-SBA-15 respectively) were prepared according to such procedures.

2.2 Methane Cracking to Grow Carbon Microfibers

The carbon microfibers were produced according to the following procedures: The 0.5 g of Co-SBA-15 catalyst was loaded in a tubular stainless steel reactor. Pure N_2 (30 ml/min.) was flowed into the reactor to purge the catalyst at 600 °C for 2 h. H_2 ($H_2/N_2 = 1/4$, v/v; 30 ml/min.) was introduced into the reactor to reduce the catalyst at 800 °C for 3 h. A mixed gas of CH_4, H_2 and N_2 ($CH_4/H_2/N_2 = 5/5/90$, v/v/v; 30 ml/min.) was passed through the catalyst for methane cracking at desired temperatures. After cracking, the methane gas was switched off and the reactor was cooled down in the H_2/N_2 atmosphere to room temperature. The influent and effluent gases were analyzed by GC on line.

2.3 Characterization

Crystallographic information of carbon microfibers was investigated with powder X-ray diffraction (XRD) (Shimadzu 6000) using filtered Cu Kα radiation as the X-ray source ($\lambda = 1.5406$ Å). High resolution transmission electron microscope (HRTEM) (JEOL 3000F FEGTEM), transmission electron microscope (TEM) (JEOL, JEM

2010) and field emission scanning electron microscope (FESEM) (JEOL, JSM 7600F) were used to observe the morphologies of Co-SBA-15 and carbon microfibers. Laser Raman spectra were recorded using a Nicolet 560 FT Raman spectrometer with a He–Ne laser operating at a power of 1 mW.

3 Results and Discussion

Figure 1a–d show the TEM images of catalysts of $Co_{0.5}$-SBA-15, Co_1-SBA-15, Co_2-SBA-15 and Co_3-SBA-15, respectively after being reduced in hydrogen at 600 °C. The black dots are the cobalt particles. They are dispersed and localized in the SBA-15 matrix. The sizes of cobalt particles are from several to 10 nm and seem bigger at the higher cobalt loading. The cobalt nano particles are densely dispersed and formed clusters. Figure 1e is the HRTEM image of the hydrogen-reduced Co_3-SBA-15. The ordered lattice structure of metal crystallite in black area can be seen. Such metallic crystallite cobalt is the active site to dissociate methane. Figure 2a–d are the FESEM images of as-synthesized carbon microfibers over the catalysts of $Co_{0.5}$-SBA-15, Co_1-SBA-15, Co_2-SBA-15 and Co_3-SBA-15, respectively by cracking methane at 800 °C for 2 h. The carbon microfibers are quite straight. The diameter of microfibers are ca. 1, 2, 4 and 6μm, respectively, same order as the concentration of cobalt doped in SBA-15. We assume that the cobalt clusters agglomerated to bigger particles during methane cracking at temperatures of 800 °C. The structure of SBA-15 is fragile at 800 °C. Figure 3a–c are the FESEM images of carbon microfibers

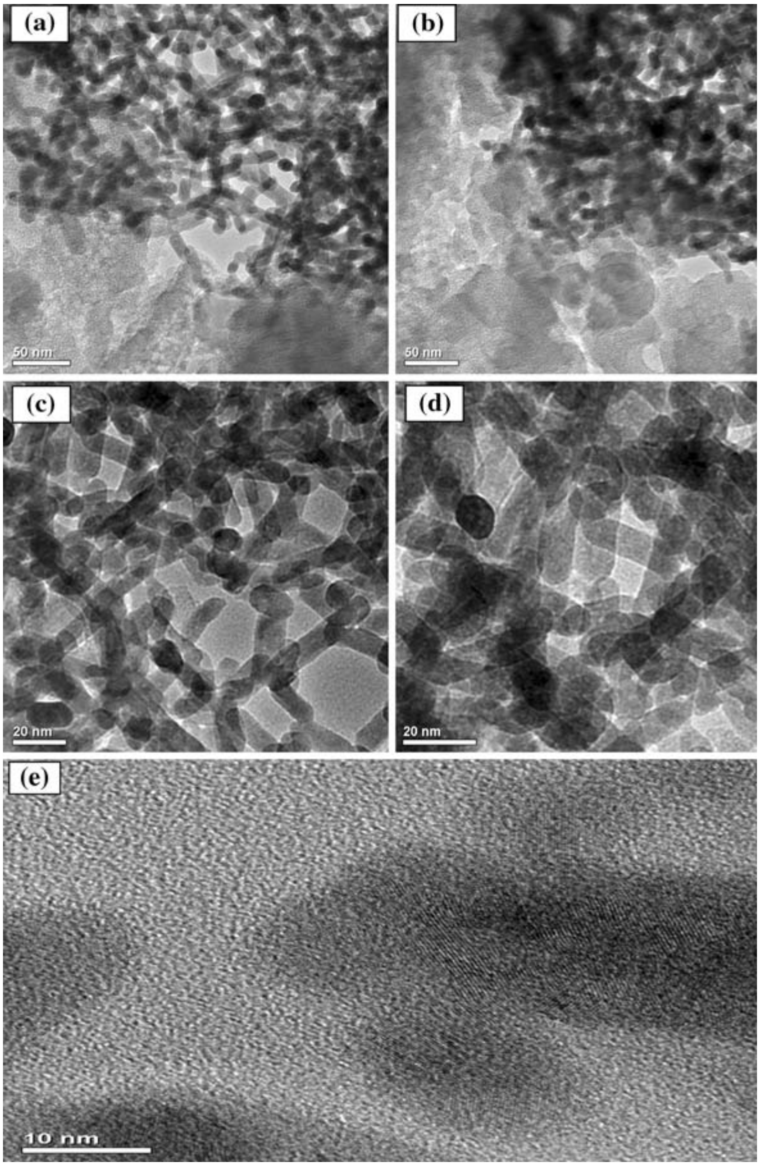

Fig. 1 TEM images of (**a**) $Co_{0.5}$-SBA-15, (**b**) Co_1-SBA-15, (**c**) Co_2-SBA-15 and (**d**) Co_3-SBA-15 after being reduced in hydrogen at 600 °C, (**e**) HRTEM of Co_3-SBA-15 after being reduced in hydrogen at 600 °C

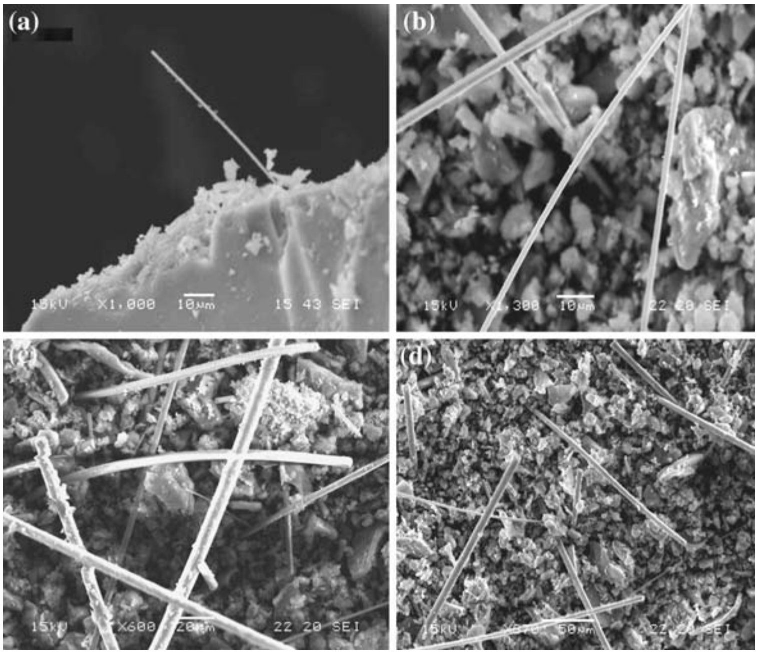

Fig. 2 FESEM images of carbon microfibers obtained over (**a**) $Co_{0.5}$-SBA-15, (**b**) Co_1-SBA-15, (**c**) Co_2–SBA-15 and (**d**) Co_3-SBA-15 by cracking methane at 800 °C for 2 h

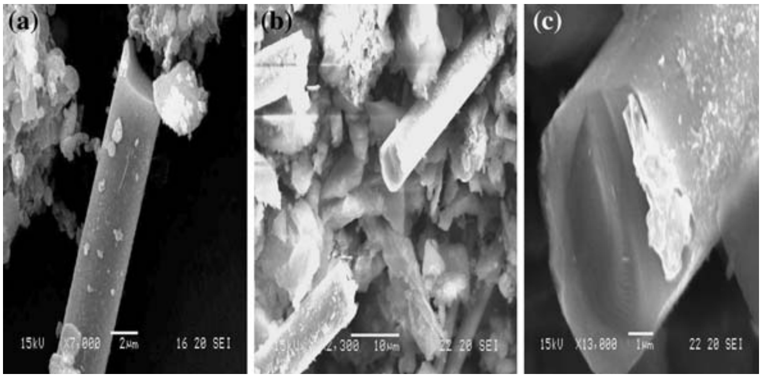

Fig. 3 FESEM images of tips of carbon microfibers obtained over (**a**) Co_1-SBA-15, (**b**) Co_2-SBA-15 and (**c**) Co_3-SBA-15 by cracking methane at 800 °C for 1 h

collected from methane cracking over the catalysts of Co_1-SBA-15, Co_2-SBA-15 and Co_3-SBA-15 at 800 °C for 1 h respectively. It is clear that the carbon fibers are solid rods rather than hollow tubes. We can not observe the catalyst particles on the carbon fiber tips. Thus we speculate that the Co catalytic particles are immobilized in SBA-15. During methane cracking, carbon is initially nucleated on the Co particles. The carbon fibers are always exposed to the methane gas. Carbon microfibers are grown through the interaction of Co metal catalysts at the root with methane vapor. In general, as to nanotubes, the catalyst might stay at the growing end of the nanofibre (called tip growth), or it might sit at the starting end (root growth). The particle size and fiber diameter are similar [22, 23]. In most case, multiwalled carbon nanotubes follow the tip growth mechanism in which the Co particles are present at the tips of the MWCNTs as an active site for growth. In the catalyst of Co-SBA-15, we got large straight microfibers. When we increased the cobalt concentration up to 5 wt%, we only harvested carbon particles rather than fibers or tubes. Quite how the microfiber forms is still unknown. It is clear that the carbon accumulation follows the root-growth mechanism while not tip-growth.

Figure 4 shows the carbon microfibers obtained over the Co_2-SBA-15 sample at 600 °C for 1 h. The carbon fibers are about 12 nm in diameter. It is clear that the carbon fibers grow from inside Co_2-SBA-15. We could not observe the nano metal catalyst particles on the tips of nanofibers as well. We deduce that at low temperature and in the initial step, the fiber is actually growing over the isolated nanometal catalyst and the fiber is nanosized. When the reaction temperature was elevated, the fiber was grown thicker and thicker and finally reached micro scale in diameter.

Figure 5 shows the methane conversion as a function of cracking temperature over the catalysts of $Co_{0.5}$-SBA-15, Co_1-SBA-15, Co_2-SBA-15 and Co_3-SBA-15. When the cobalt concentration is as low as 0.5 wt%, the methane

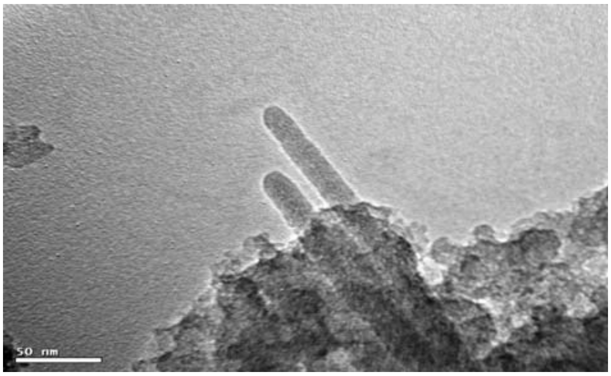

Fig. 4 FESEM image of carbon nanofibers obtained over Co_2-SBA-15 by cracking methane at 600 °C for 1 h

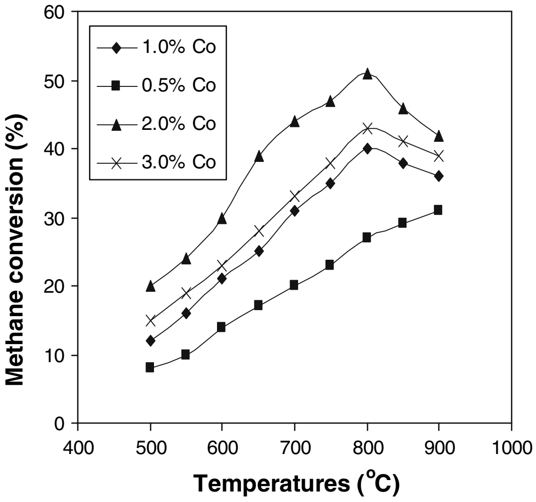

Fig. 5 Methane conversion versus reaction temperatures over Co-SBA-15 catalysts

conversion is linearly dependent on the reaction temperature. When the cobalt loading are up to 1, 2 and 3 wt%, the maximum methane conversions on each catalyst are all obtained at the temperature of 800 °C. Amongst the four series catalysts in the temperature ranging from 500 to 900 °C, the catalyst Co_2-SBA-15 always shows the highest methane conversion and at 800 °C it reaches 53.0%.

The formation of carbon nanotubes by the methane decomposition over the Co catalysts supported on several other supports (MgO, Al_2O_3, SiO_2, and TiO_2) has been investigated. The catalytic activity was strongly dependent on the type of support. The cobalt metal particles with diameters from 10 to 30 nm grew carbon nanotubes from methane preferentially, while ones larger than 30 nm were inactive for the reaction. The Co metals were present at the tip or in the hollow of MWNT. The carbon tubes were not straight [35]. Over the iron catalysts, methane (CH_4/H_2 = 30/70, v/v) cracking at 1150 and 1075 °C produced relatively straight carbon microfibers (diameter: ca. 10 μm) and coiled fibers (diameter: ca. 0.5 μmS) respectively. 10% methane diluted in 90% hydrogen at 1150 °C produced coiled fibers (diameter: ca. 1 μm). The growth of the microfibers was very sensitive to the reaction conditions which can be tuned to produce either microfibers or fibers rather in the nanometer range. When lowering the reaction temperature down to 1075 °C, fibers with diameters of several hundred nanometers were obtained [15]. Over this catalyst, catalytic decomposition occurred at about 997 °C, whereas the pyrolysis of methane dominated at higher temperatures leading to a core-and-shell structure of the fibers. To prolong cracking time of methane (CH_4/H_2 = 30/70) at 1150 °C for 8 h resulted in the formation of fibers with diameter more than 20 μm and length approaching a limit of 40 mm. The detailed mechanism was not studied. Over the Co-SBA-15 catalysts, when we elevated the reaction temperatures to 1150 °C, neither carbon nanotubes nor microfibers were created. We think that at such temperature the structure of SBA-15 has already been demolished. We also found that increasing the methane concentration was not good at producing uniform carbon microfibers over the Co-SBA-15 catalysts.

The yields of carbon microfibers at reaction temperature of 800 °C over 0.5 g catalyst for 8 h are listed in Table 1. The yield keeps the order of Co_2-SBA-15 > Co_3-SBA-15 > Co_1-SBA-15 > $Co_{0.5}$-SBA-15. The cobalt concentration is not the higher the better for the carbon production. Acetylene decomposition over the catalysts of Co/MgO (Co loading: 10–75%) for the formation of carbon nanotubes has been studied. The yield of MWNTs increased with an increase in Co loading (up to 50%). Active Co nanoparticles (12–18 nm) were responsible for the growth of coiled-like MWNTs [36]. SWNTs have been synthesized over the Co-MCM-41 catalysts by CO disproportionation. Increasing the cobalt loading could be used to increase the yield of the SWNT, but cobalt loadings larger than 3 wt% altered the uniformity of the diameter distribution of the SWNT produced. Cobalt clusters with an optimal size of approximately 6–8 Å led to the growth of SWNT with uniform diameter. The lowest 0.5 wt% cobalt loading in MCM-41 produced just a few Co clusters in the sample large enough to grow SWNT. The highest (4 wt%) cobalt concentration produced large cobalt particles, which led to the growth the graphite. If the cobalt was not initially strongly stabilized in the MCM-41 framework, the catalyst could not produce SWNT with narrow diameter distribution. Incorporation of up to 3 wt% Co in MCM-41 produced anchored small clusters and SWNTs with a narrow diameter distribution [37]. MCM-41 and SBA-15 are two most important mesoporous materials. The pores in MCM-41 are smaller than those in SBA-15. The larger porous structures of SBA-15 are easier to be demolished at higher

Table 1 The carbon yield over 0.5 g of catalyst by methane cracking at 800 °C for 8 h

Catalysts	$Co_{0.5}$-SBA-15	Co_1-SBA-15	Co_2 –SBA-15	Co_3-SBA-15
Carbon yield (g)	0.085	0.106	0.147	0.125

temperatures. As shown in Fig. 1 no angstrom scaled particles were generated in Co-SBA-15 materials, so we obtained microfibers rather than nanotubes. The cobalt particles are strongly localized in the SBA-15 substrate so we can not detect them on the carbon fiber tips. The cobalt loading amount in both MCM-41 and SBA-15 can be low as 0.5 wt% but cannot exceed 4 wt% for producing either nanotubes or microfibers.

Figure 6a and b are the FESEM images of carbon microfibers obtained over the catalysts of Co_1-SBA-15 and Co_2-SBA-15 respectively by methane cracking at 800 °C for 8 h. From the images the carbon microfibers at least several hundreds micrometers in length can be observed. During FESEM observation, we estimated that some microfibers were about 2 mm in length.

Over the 0.5 g of catalyst Co_2-SBA-15, we studied the dependence of reaction time on the fibers yield and the results are listed in Table 2. The carbon yield is growing up until at the 16th hours. We observed that lasting the reaction time longer than 16 h was not able to make the carbon microfibers grow continuously, indicating that the catalyst has been deactivated. When the reaction time was longer than 16 h, further reaction did not prolong the carbon microfibers any more. This result demonstrates that the carbon microfibers actually came from the catalytic cracking of methane rather than thermal pyrolysis.

The XRD pattern of as synthesized carbon microfibers over the catalyst Co_2-SBA-15 at 800 °C for 8 h is shown in Fig. 7. A strong diffraction peak at 2 θ of 26.36 is observed. This is the identical peak of graphitic carbon, indicating that the carbon microfibers are graphitic. Figures 8a and b are the HRTEM images of the carbon microfibers obtained over the catalysts of $Co_{0.5}$-SBA-15 and Co_2-SBA-15 by the cracking of methane at 800 °C for 8 h respectively. There are mainly three types of carbon nanofibers (CNFs): the fishbone or herringbone CNFs, platelet CNFs and the ribbon CNFs [38]. In Fig. 8a and b, the fringes of graphite sheets are clearly observed. No

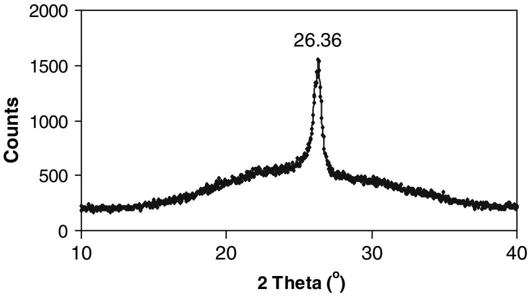

Fig. 7 XRD pattern of carbon microfibers obtained over Co_2-SBA-15 by methane cracking at 800 °C for 8 h

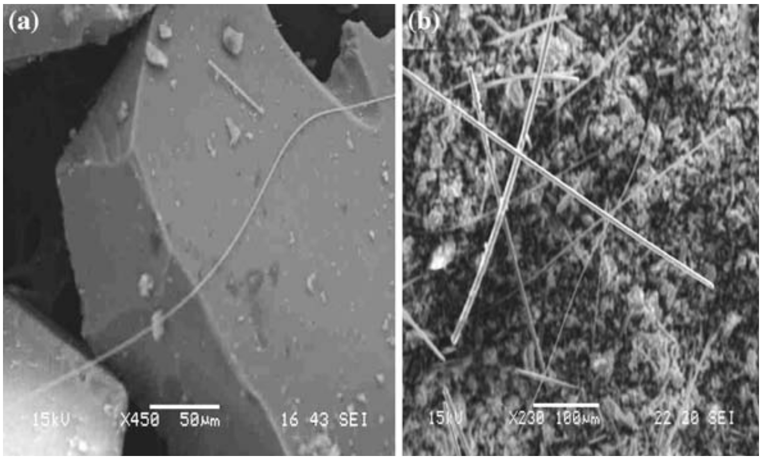

Fig. 6 FESEM images of carbon microfibers obtained over (**a**) Co_1-SBA-15 and (**b**) Co_2-SBA-15 by methane cracking at 800 °C for 8 h

Table 2 The carbon yield over 0.5 g of Co_2-SBA-15 catalyst by methane cracking at 800 °C

Reaction time (h)	2	4	6	8	10	12	14	16
Carbon yield (g)	0.043	0.077	0.105	0.147	0.160	0.171	0.175	0.175

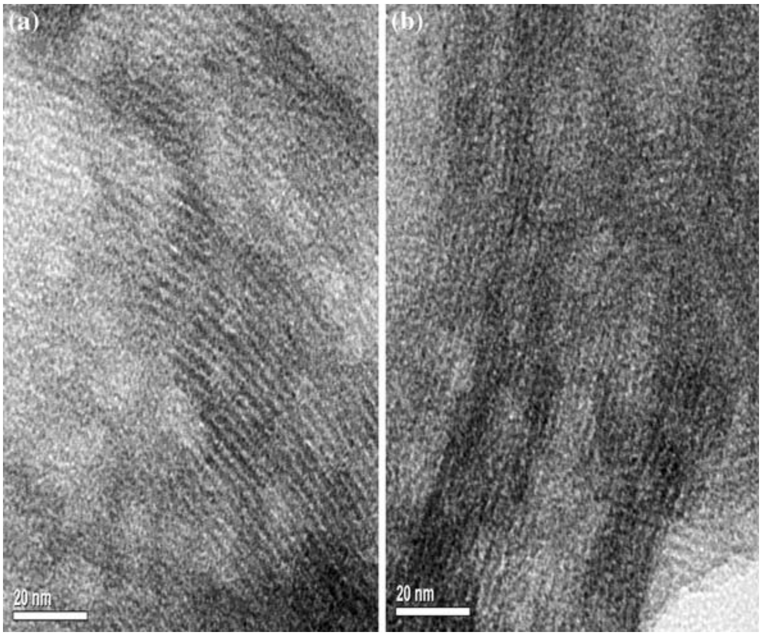

Fig. 8 HRTEM images of carbon microfibers obtained over (**a**) $Co_{0.5}$-SBA-15 and (**b**) Co_2-SBA-15 by methane cracking at 800 °C for 8 h

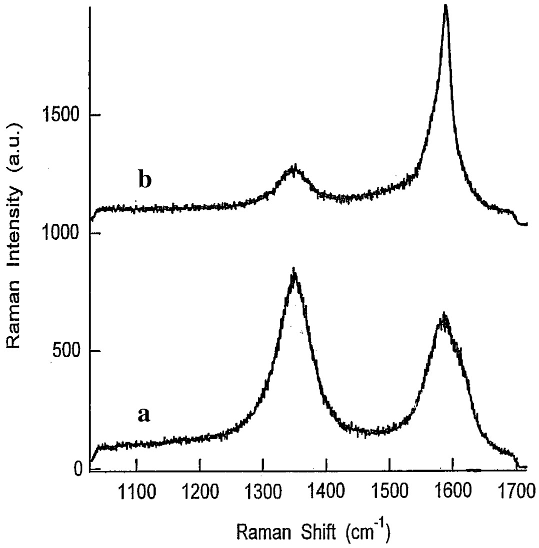

Fig. 9 Raman spectra of carbon microfibers obtained over (**a**) Co_2-SBA-15 and (**b**) $Co_{0.5}$-SBA-15 by methane cracking at 800 °C for 8 h

hollow tube structures can be detected. There are many defects in the graphitic sheets. The graphene layers in Fig. 8a are more ordered than those in Fig. 8b. The graphene layer seems in herringbone structure. The outer graphitic structures in Fig. 8b are more complicated. The graphene layers exist in several orientations. Some people considered that the outer graphitic sheets are caused by non-catalytic thickening of CNTs [39].

Figure 9a and b are the Raman spectra of the carbon microfibers obtained over the catalysts of Co_2-SBA-15 and $Co_{0.5}$-SBA-15 by cracking methane at 800 °C for 8 h respectively. The band at 1568 cm^{-1} is the one exhibited by highly ordered graphite and is therefore designated as G band. The band at 1341 cm^{-1} is attributed to the defect in graphite and is therefore designated as D band. The integrated intensity of the D and G bands (I_D, I_G) is generally used to evaluate the structural order of carbon fibers, i.e., a lower value of the ratio of I_D/I_G indicates a higher degree of structural order [40]. The D band in the spectrum of Fig. 9a is stronger than that in the Fig. 9b while the G band in Fig. 9a is weaker than in Fig. 9b. This result indicates that the carbon microfibers obtained over the catalyst of Co_2-SBA-15 are of more defects than those obtained over the catalyst of $Co_{0.5}$-SBA-15. In other words, the graphitic level of the carbon fiber (thin fiber) obtained over the catalyst of $Co_{0.5}$-SBA-15 is higher than that (thick fiber) obtained over the catalyst of Co_2-SBA-15.

4 Conclusion

(i) Co-SBA-15 (Co: 0.5, 1, 2, 3 wt%) catalysts were prepared by hydrothermal synthesis process.
(ii) Methane cracking over Co-SBA-15 catalysts produced straight carbon microfibers. The carbon microfibers were graphitic. Over the catalyst of 2 wt% Co loaded SBA-15 at 800 °C, we harvested the maximum amount of carbon microfibers. The concentration of cobalt loaded in SBA-15 influenced the diameter of microfiber.
(iii) The fiber production followed the root-growth mechanism. At low temperature (600 °C), carbon

nanofibers were created while at high temperature (800 °C), microfibers were generated.

(iv) The carbon microfiber grown over the catalyst of $Co_{0.5}$-SBA-15 had a higher degree of graphitic structural order than that obtained over the catalyst of Co_2-SBA-15.

Acknowledgments We gratefully acknowledge the financial support under an A*STAR SERC Grant (A*STAR project no: 0221010035).

References

1. Hughes TV, Chambers CR, US patent 405480 (1889)
2. Schützenberger P, Schützenberger L (1890) CR Acad Sci Paris 111:774
3. Pelabon C, Pelabon H (1903) CR Acad Sci Paris 137:706
4. De-Jong KP, Geus JW (2000) Catal Rev Sci Eng 42(4):481
5. Serp P, Corrias M, Kalck P (2003) Appl Catal A 253(2):337
6. Hillert M, Lange N (1958) Zeitschr Kristall 111:24
7. Robertson SD (1969) Nature 221:1044
8. Murayama H, Maeda T (1990) Nature 345:791
9. Baird T, Fryer JR, Grant B (1971) Nature 233(5318):329
10. Lijima S (1991) Nature 354:56
11. lijima S, Ichihashi T (1993) Nature 363:603
12. Bethune DS, Kiang CH, de Vries MS, Gorman G, Savoy R, Vasquez J, Bayers R (1993) Nature 363:605
13. Tibbetts GG (1989) Carbon 27:745
14. Bubert H, Ai X, Haiber S, Heintze M, Brüser V, Pasch E, Brandl W, Marginean G (2002) Spectrochimica Acta Part B 57:1601
15. Schlüter OFK, Wehner BI, Hu D, Xia W, Quandt T, Marginean G, Brandl W, Muhler M (2004) Appl Catal A 274:71
16. Liu BC, Gao LZ, Liang Q, Tang SH, Qu MZ, Yu ZL (2001) Catal Lett 71:225
17. Liang Q, Gao LZ, Li Q, Tang SH, Liu BC, Yu ZL (2001) Carbon 39:897
18. Li H, Li Q, Gao LZ, Au CT, Yu ZL (2001) Catal Lett 74:185
19. Zhou LP, Ohta K, Kuroda K, Ni L, Gao LZ, Matsumoto T, Nakamura J (2005) J Phys Chem B 109:4439
20. Cuong PH, Vieira R, Louis B, Carvalho A, Amadou J, Dintzer T, Ledoux MJ (2006) J Catal 240:194
21. Qian W, Liu T, Wei F, Wang Z, Li Y (2004) Appl Catal A 258:121
22. Ajayan PM (2004) Nature 427:402
23. Helveg S, López-Cartes C, Sehested J, Hansen PL, Clausen BS, Rostrup-Nielsen JR, Abild-Pedersen F, Nørskov JK (2004) Nature 427:426
24. Zhao DY, Feng JL, Huo QS, Melosh N, Fredrickson GH, Chmelka BF, Stucky GD (1998) Science 279(5350):548
25. Lu Q, Gao F, Komarneni S, Mallouk TE (2004) J Am Chem Soc 126: 8650
26. Bharat LN, Sridhar K, Hiroaki K (2000) Chem Commun 2389
27. Han YJ, Stucky GD, Butler A (1999) J Am Chem Soc 121(42):9897
28. Gao F, Lu QY, Liu XY, Yan YS, Zhao DY (2001) Nano Lett 1(12):743
29. Lapkin A, Bozkaya B, Mays T, Borello L, Edler K, Crittenden B (2003) Catal Today 81:611
30. Nozaki C, Lugmair CG, Bell AT, Tilley TD (2002) J Am Chem Soc 124:13194
31. Li H, Li J, Ni H, Song D (2006) Catal Lett 110(1–2):71
32. Lu AH, Li WC, Schmidt W, Kiefer W, Schüth F (2004) Carbon 42:2939
33. Kónya Z, Molnar E, Tasi G, Niesz K, Somorjai GA, Kiricsi I (2007) Catal Lett 113(1–2):19
34. Somanathan T, Pandurangan A, Sathiyamoorthy D (2006) J Mol Catal A 256:193
35. Takenaka S, Ishida M, Serizawa M, Tanabe E, Otsuka K (2004) J Phys Chem B 108:11464
36. Singh BK, Ryu H, Chikate RC, Hoa ND, Park SJ, Kim S, Lee JR (2006) Solid State Commun 139:102
37. Chen Y, Ciuparu D, Lim S, Haller GL, Pfefferle LD (2006) Carbon 44:67
38. Zhu YA, Shui ZJ, Zhao TJ, Dai YC, Cheng ZM, Yuan WK (2005) Carbon 43:1694
39. Huh Y, Lee JY, Cheon J, Hong YK, Koo JY, Lee TJ, Lee CJ (2003) J Mater Chem 13:2297
40. Darmstadt H, Sümmchen L, Ting JM, Roland U, Kaliaguine S, Roy C (1997) Carbon 35:1581